THE ASTROPHYSICAL JOURNAL, 567:L103–L106, 2002 March 10

CONSTRAINTS ON REIONIZATION FROM THE THERMAL HISTORY OF THE INTERGALACTIC MEDIUM[1,2]

TOM THEUNS,[3] JOOP SCHAYE,[4] SALEEM ZAROUBI,[5] TAE-SUN KIM,[6] PANAYIOTIS TZANAVARIS,[3] AND BOB CARSWELL[3]

Received 2001 October 31; accepted 2002 February 1; published 2002 February 15

ABSTRACT

The temperature of the diffuse, photoheated intergalactic medium (IGM) depends on its reionization history because the thermal timescales are long. The widths of the hydrogen Lyα absorption lines seen in the spectra of distant quasars that arise in the IGM can be used to determine its temperature. We use a wavelet analysis of the Lyα forest region of quasar spectra to demonstrate that there is a relatively sudden increase in the line widths between redshifts $z \approx 3.5$ and 3.0, which we associate with entropy injection resulting from the reionization of He II. The subsequent falloff in temperature after $z \approx 3.5$ is consistent with a thermal evolution dominated by adiabatic expansion. If, as expected, the temperature also drops rapidly after hydrogen reionization, then the high temperatures inferred from the line widths before He II reionization imply that hydrogen reionization occurred below redshift $z = 9$.

Subject headings: cosmology: observations — cosmology: theory — galaxies: formation — intergalactic medium — quasars: absorption lines

1. INTRODUCTION

Neutral hydrogen in the intergalactic medium (IGM) along the line of sight to quasars (QSOs) at redshifts $z \lesssim 6$ produces hundreds of Lyα absorption lines. The fact that not all flux is absorbed (i.e., the absence of a "Gunn-Peterson" trough; Gunn & Peterson 1965) requires that the universe be ionized to a far higher level than can be attributed to residual ionization from recombination. At lower redshifts ($z \lesssim 3$), *observed* stars and QSOs produce enough ionizing photons to explain the high levels of ionization, but the nature of the sources responsible for converting most of the IGM from neutral to ionized remains uncertain, as does the epoch of reionization (e.g., Barkana & Loeb 2001).

The observed mean flux decrement D_A blueward of the QSO's Lyα emission line increases with the redshift of the quasar, both because the intensity of the ionizing background radiation decreases above $z = 4$ (e.g., McDonald & Miralda-Escudé 2001) and because the mean density $\bar{\rho}$ of the universe—and hence the neutral fraction $x \propto \bar{\rho} T^{-0.7}/\Gamma_{\rm H\,I}$ for fixed values of the photoionization rate $\Gamma_{\rm H\,I}$ and temperature T—increases. Recently, Becker et al. (2001) and Djorgovski et al. (2001) observed a sudden increase in D_A in the spectra of redshift $z \sim 6$ QSOs discovered by the Sloan Digital Sky Survey. Such a sharp rise has been predicted to mark the transition associated with a sudden epoch of reionization (e.g., Cen & Ostriker 1993; Gnedin 2000). Similarly, a sudden increase in the He II opacity has been detected around $z \sim 3$ (Reimers et al. 1997; Heap et al. 2000; Kriss et al. 2001), associated with helium reionization.

Another way to study the reionization history of the IGM is to investigate its thermal evolution. Because its cooling time is long, the low-density IGM retains some memory of when and how it was reionized (e.g., Miralda-Escudé & Rees 1994; Hui & Gnedin 1997; Haehnelt & Steinmetz 1998). The combined effects of photoionization heating and adiabatic expansion introduce a tight temperature-density relation in the unshocked IGM, which can be approximated by a power law $T = T_0(\rho/\bar{\rho})^{\gamma-1}$ for densities around the cosmic mean (Hui & Gnedin 1997). A change in these parameters influences the shapes of the Lyα lines because thermal broadening and Jeans smoothing determine the line widths (e.g., Theuns, Schaye, & Haehnelt 2000). Schaye et al. (1999) used hydrodynamic simulations to demonstrate that one can accurately calibrate the relation between the minimum line width b as a function of column density ($N_{\rm H\,I}$) on the one hand and the underlying T-ρ relation on the other. Schaye et al. (2000) applied the method to observations in the redshift range 2.0–4.5 and found that T_0 peaks at $z \sim 3$, which they interpreted as evidence for the reionization of He II. Ricotti, Gnedin, & Shull (2000) used pseudohydrodynamic simulations and found a similar temperature increase, albeit only at the 0.5 σ level. McDonald et al. (2001) found no evidence for temperature evolution, but their analysis neglected the important temperature dependence of Jeans smoothing. Finally, the analysis of Zaldarriaga, Hui, & Tegmark (2001) neglected hydrodynamic effects altogether.

Here we provide new evidence for a relatively sudden increase in T_0 between redshifts $z \approx 3.5$ and 3.0, using a new method based on a wavelet decomposition of the absorption spectrum. We then use the measured values of T_0 at higher redshift to constrain the epoch of hydrogen reionization $z_{\rm H}$ and find that the data require $z_{\rm H} \lesssim 9$ for any reasonable value ($T_0 \lesssim 6 \times 10^4$ K) of the hydrogen reionization temperature.

2. HELIUM REIONIZATION

2.1. *Wavelet Analysis*

Our analysis uses wavelets to characterize line widths. By picking an appropriate wavelet scale (we used ~15 km s^{-1}), we find that the amplitude A of the wavelet anticorrelates with

[1] Based on observations made at the W. M. Keck Observatory, which is operated as a scientific partnership between the California Institute of Technology and the University of California; it was made possible by the generous support of the W. M. Keck Foundation.

[2] Based on public data released from the Very Large Telescope/UV-Visual Echelle Spectrograph Commissioning and Science Verification and from the OPC program 65.O-296A (PI S. D'Odorico) at the Very Large Telescope/Kueyen Telescope, European Southern Observatory, Paranal, Chile.

[3] Institute of Astronomy, Madingley Road, Cambridge CB3 0HA, UK.

[4] School of Natural Sciences, Institute for Advanced Study, Einstein Drive, Princeton NJ 08540.

[5] Max-Planck Institut für Astrophysik, Karl-Schwarzschild-Strasse 1, Postfach 1317, Garching D-85741, Germany.

[6] European Southern Observatory, Karl-Schwarzschild-Strasse 2, Garching D-85748, Germany.

the widths of the lines—and hence the temperature T_0 of the absorbing gas, $\langle A\rangle \propto T_0^{-1}$. By examining the statistics of A along the spectrum, we can look for changes in temperature in an objective way, given that the wavelet decomposition is unique. Full details can be found in Theuns & Zaroubi (2000) and Theuns et. al (2002); here we give only a brief summary of the underlying reasoning.

To investigate whether a region of a given size V of the QSO spectrum has an unusual temperature, we compare the cumulative probability distribution $C_V(A)$ of the wavelet amplitudes in that region, with $C(A)$ for the spectrum as a whole. If the region is unusually hot, it will tend to have very few large wavelet amplitudes, and hence the maximum difference $\Delta(V) = C_V - C$ will be large (note that by construction, $|\Delta| \leq 1$, and it is defined for a given *region*). Conversely, cold regions will have large, negative $\Delta(V)$. In Figure 1*a*, we have plotted Δ for regions of 5000 km s^{-1} along a mock spectrum of a simulation.[7] The mock spectrum has a jump in T_0 from 2.2×10^4 K below redshift $z = 3.3$ to 1.5×10^4 K above it. As expected, there is a corresponding jump in Δ at $z = 3.3$, from positive values at low redshifts to negative ones at higher redshifts.

To determine whether a high value of $|\Delta|$ is statistically significant—and hence whether we have identified a region with an unusual temperature—we proceed as follows. We repeat the procedure with spectra in which the absorption lines are randomly scrambled (with replacement, see Theuns et al. 2002), in order to wash out any correlations in the wavelet amplitudes resulting from intrinsic temperature fluctuations. Using these randomized spectra, we can construct the statistical probability $P(\Delta)$ from the fraction of regions in the randomized spectra that have a given value of Δ. Given $P(\Delta)$, we can determine how likely a value of Δ—and hence of a temperature deviation—is in the original spectrum. Performing this analysis, we find that the detected change in Δ in the mock spectrum has a statistical significance of more than 99.5%, shown as the solid line in Figure 1*a* (positive values refer to regions hotter than average and vice versa for negative values). This means that in only one out of 200 random realizations do we, by chance, get values of $|\Delta| \gtrsim 0.2$. Note that we only use the simulation to generate the spectrum, not to assign the statistical significance of a change in Δ. In the preparation of the mock spectrum, we have imposed the same biases as are present in the real data, by adding noise and instrumental broadening to the simulated lines and by scaling the mean absorption to the observed value. We, therefore, believe that the method can be applied to real data with confidence.

We have applied the same wavelet analysis to high-resolution echelle spectra of Q0055−2169 (emission redshift $z_{\rm em} = 3.6$; Kim et al 2001), the combined spectrum of Q0302−003 ($z = [3, 3.27]$; Kim et al 2001) and APM 0827+5255 ($z = [3.27, 3.7]$; Ellison et al 1999), and Q1422+231 ($z_{\rm em} = 3.6$; Rauch et al 1997) (Figs. 1*b*, 1*c*, and 1*d*, respectively). In each spectrum, we find a cold region at high redshift and a hot region at lower redshift, each significant at the more than 99% level when compared to randomized spectra. Figures 1*b* and 1*c* appear very similar to the mock spectrum of Figure 1*a*, in which we had imposed a sudden temperature increase below $z = 3.3$. Note that the implied temperature evolution is exactly opposite of what one would expect from photoheating in the optically thin limit, in which case the IGM will gradually cool down. We take this as strong evidence that a large fraction of He II is reionized around redshift $z \approx 3.3$.

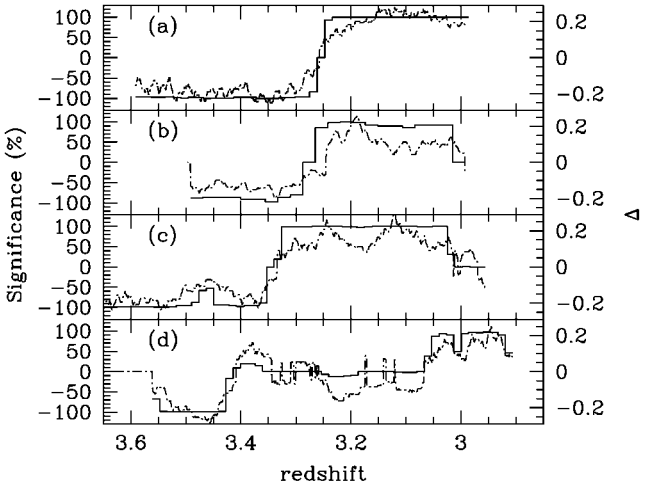

FIG. 1.—(*a–d*) Temperature statistic Δ (*right-hand scale, dot-dashed line*) and statistical significance for Δ in percent (*left-hand scale, solid line*) as a function of redshift for the mock spectrum, Q0055−2169, the combined spectrum of Q0302−003 ($z = [3, 3.27]$) and APM 0827+5255 ($z = [3.27, 3.7]$), and Q1422+231. Negative values for Δ and the significance denote cold regions and vice versa for hot regions. The mock spectrum has a jump in T_0 from 2.2×10^4 K below $z = 3.3$ to 1.5×10^4 K above $z = 3.3$. The statistical significance of the regions with a large value of $|\Delta|$ at high and low z's, when compared with randomized spectra made from this spectrum, but without a sudden temperature change, is more than 99%. The observed data exhibit a similarly significant jump, in the sense that the higher redshift halves are colder than the lower redshift halves.

The mean wavelet amplitude scales approximately inversely with temperature: $\langle A\rangle \propto T_0^{-1}$ (Theuns et al. 2002). We have used hydrodynamic simulations to calibrate the proportionality constant and investigate its dependence on γ. Applying the calibration to the above QSO sample, we obtain values for T_0 in good agreement with those obtained by Schaye et al. (2000) from the cutoff in the line width–column density relation, i.e., $T_0 \approx 10^{4.1}$ at $z \geq 3.4$ and $T_0 \approx 10^{4.3}$ at $z \approx 3.0$. This assumes the value of γ as determined by Schaye et al., but reasonable changes in γ do not change T_0 by more than ~10% (Theuns et al. 2002). Simulations that include radiative transfer are required to investigate whether such a temperature change is consistent with He II reionization.

Other heating mechanisms, e.g., shock heating by galactic winds, do not have a major influence on the value of T_0 deduced from fitting the cutoff in the b-$N_{\rm H\,I}$ diagram, at least as long as the volume fraction of shocked gas remains small. This is because the method is based on identifying the *narrowest* lines in a region, irrespective of whether there is also a set of much broader lines. In contrast, the wavelet method used here examines *all* lines in a stretch of spectrum. So the fact that both methods find similar values for T_0 suggests that photoheating is indeed the dominant heating mechanism and that the volume filling factor of gas that has been shocked by winds is small.

2.2. *Thermal Evolution*

After reionization, the evolution of T_0 is given by

$$\frac{1}{T_0}\frac{dT_0}{dt} - \frac{1}{\mu}\frac{d\mu}{dt} = -2H + \frac{\mu\Delta_\epsilon}{(3/2)k_{\rm B}T_0}, \qquad (1)$$

[7] The cosmological parameters for this vacuum-energy–dominated, flat, cold dark matter smoothed particle hydrodynamics (SPH) simulation are (Ω_m, Ω_Λ, $\Omega_b h^2$, h, σ_8) = (0.3, 0.7, 0.01 9, 0.65, 0.9). The simulation box is 12 h^{-1} Mpc on a side, and gas and dark matter are represented with 256^3 particles each.

where H is the Hubble parameter, k_B is Boltzmann's constant, μ is the mean molecular weight, and Δ_ϵ is the effective radiative cooling rate (in units of ergs g^{-1} s^{-1}). The Δ_ϵ is negative (positive) for net cooling (heating) and includes photoelectric heating and cooling via recombination, excitation, inverse Compton scattering, collisional ionization, and bremsstrahlung (we use the rates listed in Appendix B of Theuns et al. 1998). For gas around the mean density, the dominant cooling process is the adiabatic expansion of the universe (the first term on the right-hand side of eq. [1]), except at $z > 7$, where inverse Compton cooling off the cosmic microwave background is more efficient. The radiative heating and cooling rates depend on the ionization balance of the gas, which itself depends on the temperature. By coupling equation (1) to the differential equations for the ionization balance (listed in Appendix B of Theuns et al. 1998), we can thus solve for the evolution of T_0 given a model for the ionizing background, an initial value for T_0, and the initial ionization state. We have tested this procedure using full hydrodynamic simulations and find that the evolution of T_0 is reproduced very well.

We assume the universe to be permeated by a uniform UV background with a power-law spectral shape,

$$J = \begin{cases} J_{\rm H\,I}\left(\dfrac{\nu}{\nu_{\rm H\,I}}\right)^{-1.8}, & \nu < \nu_{\rm He\,II} \text{ ergs s}^{-1}\text{ cm}^{-2}\text{ sr}^{-1}\text{ Hz}^{-1}, \\ J_{\rm He\,II}\left(\dfrac{\nu}{\nu_{\rm H\,I}}\right)^{-1.8}, & \nu \geq \nu_{\rm He\,II} \text{ ergs s}^{-1}\text{ cm}^{-2}\text{ sr}^{-1}\text{ Hz}^{-1}, \end{cases} \quad (2)$$

where $\nu_{\rm H\,I}$ is the H I ionization threshold (note that we allow for a step between the intensities of H I and He II ionizing photons but normalize $J_{\rm He\,II}$ at the hydrogen ionization edge). We set $J_{\rm H\,I} = 4 \times 10^{-23}$, which yields a photoionization rate of $\Gamma_{\rm H\,I} = 10^{-13}$ s^{-1}, and vary $J_{\rm He\,II}$ (and the corresponding ionization rate $\Gamma_{\rm He\,II}$) as described below. Because the photoheating rate is independent of the amplitude of the UV background as long as the gas is highly ionized, the exact value of $J_{\rm H\,I}$ after hydrogen reionization is unimportant. Since He II is not always highly ionized, the thermal evolution does depend on $J_{\rm He\,II}$.

The predicted evolution of T_0 is compared with the data from Schaye et al (2000) in Figure 2. We assume the IGM to be in ionization equilibrium at temperature $T_0 = 10^{4.4}$ K at redshift $z = 3.4$ as a result of He II reionization. The curves emanating from the big star then show the subsequent evolution of T_0, for the following imposed UV backgrounds. The solid curve is for a constant ionizing rate of $\Gamma_{\rm H\,I} = \Gamma_{\rm He\,II} = 10^{-13}$ s^{-1} and the corresponding photoheating from all species. Increasing or decreasing $\Gamma_{\rm H\,I}$ by a factor of 10 does not change the evolution appreciably. The short- and long-dashed curves ignore the photoelectric heating from He II and from both H I and He I, respectively. Finally, the dot-dashed line ignores photoheating altogether. The measurements of Schaye et al. (2000) below $z \sim 3$ are clearly consistent with a thermal evolution dominated by adiabatic cooling.

Prior to He II reionization, some regions will already be ionized in He II by local sources. If most of the universe is reionized significantly later, then such differences in the reionization epoch will lead to spatial variations in T_0. The wavelet analysis by Theuns et al. (2002) can detect variations in T_0 on the order of 50% over a region of 5000 km s^{-1}, yet no such fluctuations were found in the data. The wavelet analysis by Zaldarriage (2001) also failed to detect any such temperature fluctuations. This suggests that the temperature increase is the result of the overall increase in the far-UV background following the percolation of He III regions, which prior to reionization are too small to be detected by current methods.

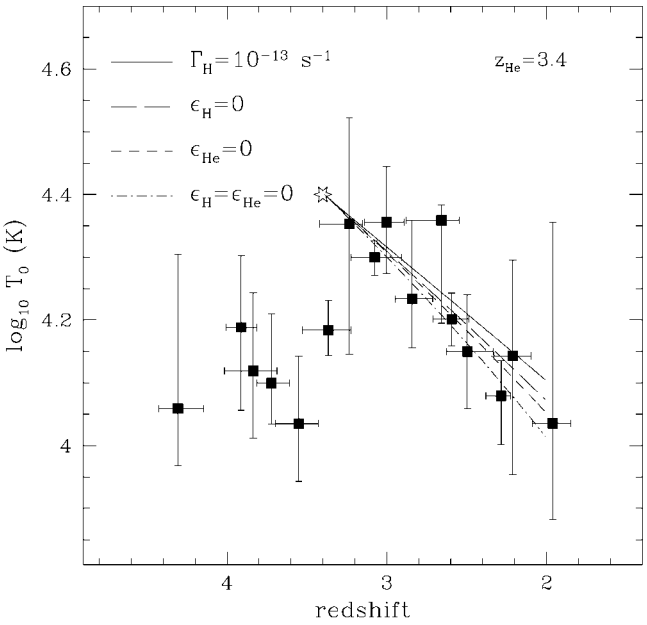

FIG. 2.—Temperature evolution of the IGM after $z = 3.4$. The filled squares with error bars are determined from fitting the cutoff in the b-$N_{\rm H\,I}$ relation (Schaye et al 2000). The curves emanating from the star all assume that $T_0 = 10^{4.4}$ K at $z = 3.4$, as a result of He II reionization, and differ in the assumed UV background at lower redshifts. The solid curve includes the photoheating from H I, and from both He I and He II. The short-dashed curve neglects heating from He II, the long-dashed curve neglects heating from both H I and He I, and finally the dot-dashed curve ignores photoheating altogether. All models fitted the inferred temperature evolution extremely well.

3. HYDROGEN REIONIZATION

Given the success in reproducing the $z < 3.4$ temperature evolution, we now turn to higher redshifts. Abel & Haehnelt (1999) performed radiative transfer calculations of the expansion of an ionization bubble around a QSO and found typical temperatures of 4×10^4 K following reionization, *including* He II reionization. To put a conservative upper limit on the hydrogen reionization redshift $z_{\rm H\,I}$, we assume a higher value of $T_0 = 6 \times 10^4$ K. Assuming the gas to be in ionization equilibrium just after reionization, we compute $T_0(z)$ for a given $z_{\rm H\,I}$ as before. In Figure 3 the predicted thermal evolution for various values of $z_{\rm H\,I}$ is compared with the data.

The temperature decreases rapidly with decreasing redshift because at these temperatures, photoheating cannot compensate for the rapid expansion cooling. Consequently, *the temperature drops quickly below the values measured at $z \sim 4$, unless hydrogen reionization occurred relatively recently*. The solid curves in Figure 3 represent $\Gamma_{\rm H\,I} = 10^{-13}$ s^{-1} and a range of reionization redshifts, as indicated in the figure. For $z_{\rm H} = 6.2$, we show $\Gamma_{\rm H\,I} = 10^{-14}$ s^{-1} for comparison. The models with late H I reionization, $z_{\rm H} \leq 8$, fit the data best. Models with $z_{\rm H} \geq 9$ have $z \sim 4$ temperatures that are significantly below the measured values. For example, the $z_{\rm H} = 9.2$ curve has a reduced χ^2 of 4.5 for the five $z > 3.4$ data points.

The contribution from He II photoheating at $z \geq 5$ is uncertain. It is likely that stars dominate the H I ionizing background

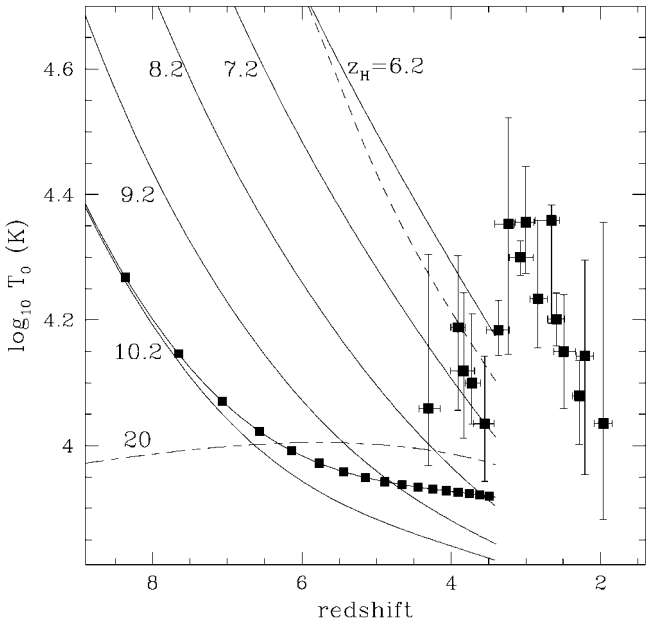

FIG. 3.—Temperature evolution of the IGM above redshift 3.4. The solid curves indicate the evolution of the temperature at the mean density for various H I reionization redshifts z_H, as indicated. The temperature after hydrogen reionization is assumed to be $T_0 = 6 \times 10^4$ K, and the hydrogen photoionization rate is $\Gamma_{H\,I} = 10^{-13}$ s^{-1} ($\Gamma_{H\,I} = 10^{-14}$ s^{-1}, *short-dashed curve*). The He II photoionization rate is adjusted so that the He III abundance is $x_{He\,III} \approx 0.1$ at $z = 3.5$. The solid curve connecting the filled squares indicates $z_H = 10.2$ and a higher He II photoionization rate, $x_{He\,III}(z = 3.5) = 0.6$. Finally, the long-dashed curves has $z_H = 20$ but a still higher He II photoionization rate, $x_{He\,III}(z = 3.5) = 0.95$. If He is mostly singly ionized at $z \gtrsim 3.5$, then the rapid decrease in T_0 after reionization places an upper limit of $z_H < 9$ on the redshift of hydrogen reionization.

at such high redshifts (e.g., Madau, Haardt, & Rees 1999) but stars emit very few He II ionizing photons. However, very massive and extremely metal-poor stars could lead to a non-negligible He II ionizing background (Tumlinson & Shull 2000). The QSO contribution is also uncertain, although the paucity of faint point sources in the Hubble Deep Field does provide some constraints (Haiman, Madau, & Loeb 1999). If He II reionized at $z \sim 3$, as argued in the previous sections, then the He III abundance, $x_{He\,III}$, should be small at higher redshifts. We, therefore, set $\Gamma_{He\,II} = 10^{-15}$ s^{-1} so that $x_{He\,III} \approx 0.1$ at redshift $z = 3.5$. This limits the plausible contribution from He II photoheating and allows us to put a conservative upper limit on the redshift of H I reionization, $z_H < 9$.

The importance of He II heating is illustrated by the solid curve connecting the filled squares. This model has $z_H = 10.2$, but the He II ionizing background is increased such that $x_{He\,III} \approx 0.6$ at $z = 3.5$. This increases T_0 ($z = 4$) significantly, although it still falls below the measured values. Finally, the long-dashed line represents a model with $z_H = 20$ and $J_{He\,II}$ further increased so that $x_{He\,III} \approx 0.96$ at $z = 3.5$. The temperature of this model is consistent with the data, yet He II is ionized at the more than 90% level as early as $z = 5$. Such a high level of ionization conflicts with the evidence (the observed He II opacities and the associated increase in T_0) that He II reionizes at $z \sim 3$.

All this leads us to the following conclusions. Two independent methods consistently find a rather sudden increase in the temperature of the IGM over the range $z \sim 3.5$–3.0, which we associate with He II reionization. If this interpretation is correct, then the He III fraction must be low at higher redshifts. Therefore, above redshifts 3.5, He II photoheating cannot be significant, and the IGM cools rapidly following H I reionization. The high values of the IGM temperature at $z \sim 4$ then require that H I reionization occurred late as well, $z_H < 9$, for any reasonable value $T_0 \lesssim 6 \times 10^4$ K for the H I reionization temperature. More plausible reionization temperatures of $T_0 \sim$
4×10^4 and 2×10^4 K would constrain the hydrogen reionization redshift further to $z_H \lesssim 8$ and $z_H \lesssim 7$, respectively.

T. T. thanks the Particle Physics and Astronomy Reasearch Council for the award of an Advanced Fellowship. J. S. is supported by a grant from the W. M. Keck Foundation. We acknowledge support from the Physics of the Intergalactic Medium network set up by the European Commission. Research was conducted in cooperation with Silicon Graphics/Cray Research utilizing the Origin 2000 supercomputer at the University of Cambridge, Department of Applied Mathematics and Theoretical Physics.

REFERENCES

Abel, T., & Haehnelt, M. G. 1999, ApJ, 520, L13
Barkana, R., & Loeb, A. 2001, Phys. Rep., 349, 125
Becker, R. H., et al. 2001, AJ, 122, 2850
Cen, R., & Ostriker, J. P. 1993, ApJ, 417, 404
Djorgovski, S. G., Castro, S. M., Stern, D., & Mahabel, A. A. 2001, ApJ, 560, L5
Ellison, S. L., Lewis, G. F., Pettini, M., Sargent, W. L. W., Chaffee, F. H., Foltz, C. B., Rauch, M., & Irwin, M. J. 1999, PASP, 111, 946
Gnedin, N. Y. 2000, ApJ, 535, 530
Gunn, J. E., & Peterson, B. A. 1965, ApJ, 142, 1633
Haehnelt, M. G., & Steinmetz, M. 1998, MNRAS, 298, L21
Haiman, Z., Madau, P., & Loeb, A. 1999, ApJ, 514, 535
Heap, S. R., Williger, G. M., Smette, A., Hubeny, I., Sahu, M. S., Jenkins, E. B., Tripp, T. M., & Winkler, J. N. 2000, ApJ, 534, 69
Hui, L., & Gnedin, N. Y. 1997, MNRAS, 292, 27
Kim, T.-S., et al. 2001, MNRAS, submitted
Kriss, G. A., et al. 2001, Science, 293, 1112
Madau, P., Haardt, F., & Rees, M. J. 1999, ApJ, 514, 648
McDonald, P., & Miralda-Escudé, J. 2001, ApJ, 549, L11
McDonald, P., Miralda-Escudé, J., Rauch, M., Sargent, W. L. W., Barlow, T. A., & Cen, R. 2001, ApJ, 562, 52
Miralda-Escude, J., & Rees, M. J. 1994, MNRAS, 266, 343
Rauch, M., et al. 1997, ApJ, 489, 7
Reimers, D., Kohler, S., Wisotzki, L., Groote, D., Rodeiguez-Pascual, P., & Warmsteker, W. 1997, A&A, 327, 890
Ricotti, M., Gnedin, N. Y., & Shull, J. M. 2000, ApJ, 534, 41
Schaye, J., Theuns, T., Leonard, A., & Efstathiou, G. 1999, MNRAS, 310, 57
Schaye, J., Theuns, T., Rauch, M., Efstathiou, G., & Sargent, W. L. W. 2000, MNRAS, 318, 817
Theuns, T., Leonard, A., Efstathiou, G., Pearce, F. R., & Thomas, P. A. 1998, MNRAS, 301, 478
Theuns, T., Schaye, J., & Haehnelt, M. G. 2000, MNRAS, 315, 600
Theuns, T., & Zaroubi, S. 2000, MNRAS, 317, 989
Theuns, T., Zaroubi, S., Kim, T.-S., Tzanavaris, P., Carswell, R. F. 2002, MNRAS, in press (astro-ph/0110600)
Tumlinson, J., & Shull, J. M. 2000, ApJ, 528, L65
Zaldarriaga, M. 2001, ApJ, 564, 153
Zaldarriaga, M., Hui, L., & Tegmark, M. 2001, ApJ, 557, 519